Conductivity mapping of graphene on polymeric films by terahertz time-domain spectroscopy

Whelan, Patrick Rebsdorf; Huang, Deping; Mackenzie, David; Messina, Sara A.; Li, Zhancheng; Li, Xin; Li, Yunqing; Booth, Timothy J.; Jepsen, Peter Uhd; Shi, Haofei; Bøggild, Peter

Published in:
Optics Express

Link to article, DOI:
10.1364/OE.26.017748

Publication date:
2018

Document Version
Publisher's PDF, also known as Version of record

Research Article | Vol. 26, No. 14 | 9 Jul 2018 | OPTICS EXPRESS 17748
Optics EXPRESS

Conductivity mapping of graphene on polymeric films by terahertz time-domain spectroscopy

PATRICK R. WHELAN,[1,7,*] DEPING HUANG,[2,7] DAVID MACKENZIE,[1] SARA A. MESSINA,[1,3] ZHANCHENG LI,[2] XIN LI,[2] YUNQING LI,[2] TIMOTHY J. BOOTH,[1] PETER U. JEPSEN,[1,4] HAOFEI SHI,[2,5] AND PETER BØGGILD[1,6]

[1] *Center for Nanostructured Graphene (CNG), Technical University of Denmark, Ørsteds Plads 345C, DK-2800 Kongens Lyngby, Denmark*
[2]*Chongqing Institute of Green and Intelligent Technology, Chinese Academy of Sciences, 266 Fang Zheng Ave., Chongqing 400714, China*
[3]*Materials Department, University of California, Santa Barbara, CA 93106, USA*
[4]*DTU Fotonik, Technical University of Denmark, Ørsteds Plads 343, DK-2800 Kongens Lyngby, Denmark*
[5]*shi@cigit.ac.cn*
[6]*peter.boggild@nanotech.dtu.dk*
[7]*These authors contributed equally to the work*
[*]*patwhe@nanotech.dtu.dk*

Abstract: Fast inline characterization of the electrical properties of graphene on polymeric substrates is an essential requirement for quality control in industrial graphene production. Here we show that it is possible to measure the sheet conductivity of graphene on polymer films by terahertz time-domain spectroscopy (THz-TDS) when all internally reflected echoes in the substrate are taken into consideration. The conductivity measured by THz-TDS is comparable to values obtained from four point probe measurements. THz-TDS maps of 25x30 cm^2 area graphene films were recorded and the DC conductivity and carrier scattering time were extracted from the measurements. Additionally, the THz-TDS conductivity maps highlight tears and holes in the graphene film, which are not easily visible by optical inspection.

OCIS codes: (240.0310) Thin films; (300.6495) Spectroscopy, terahertz; (310.3840) Materials and process characterization; (310.6870) Thin films, other properties.

References and links

1. P. Bøggild, D. M. A. Mackenzie, P. R. Whelan, D. H. Petersen, J. C. D. Buron, A. Zurutuza, J. C. Gallop, L. Hao, and P. U. Jepsen, "Mapping the electrical properties of large-area graphene," 2D Mater. **4**(4), 42003 (2017).
2. J. L. Tomaino, A. D. Jameson, J. W. Kevek, M. J. Paul, A. M. van der Zande, R. A. Barton, P. L. McEuen, E. D. Minot, and Y.-S. Lee, "Terahertz imaging and spectroscopy of large-area single-layer graphene," Opt. Express **19**(1), 141–146 (2011).
3. J. Horng, C. F. Chen, B. Geng, C. Girit, Y. Zhang, Z. Hao, H. A. Bechtel, M. Martin, A. Zettl, M. F. Crommie, Y. R. Shen, and F. Wang, "Drude conductivity of Dirac fermions in graphene," Phys. Rev. B Condens. Matter Mater. Phys. **83**(16), 1–5 (2011).
4. I. Maeng, S. Lim, S. J. Chae, Y. H. Lee, H. Choi, and J. H. Son, "Gate-controlled nonlinear conductivity of Dirac fermion in graphene field-effect transistors measured by terahertz time-domain spectroscopy," Nano Lett. **12**(2), 551–555 (2012).
5. J. D. Buron, D. H. Petersen, P. Bøggild, D. G. Cooke, M. Hilke, J. Sun, E. Whiteway, P. F. Nielsen, O. Hansen, A. Yurgens, and P. U. Jepsen, "Graphene conductance uniformity mapping," Nano Lett. **12**(10), 5074–5081 (2012).
6. J. D. Buron, D. M. A. Mackenzie, D. H. Petersen, A. Pesquera, A. Centeno, P. Bøggild, A. Zurutuza, and P. U. Jepsen, "Terahertz wafer-scale mobility mapping of graphene on insulating substrates without a gate," Opt. Express **23**(24), 30721–30729 (2015).

#326297 https://doi.org/10.1364/OE.26.017748
Journal © 2018 Received 19 Mar 2018; revised 20 Jun 2018; accepted 21 Jun 2018; published 25 Jun 2018

Optics EXPRESS

7. H. Lin, P. Braeuninger-Weimer, V. S. Kamboj, D. S. Jessop, R. Degl'Innocenti, H. E. Beere, D. A. Ritchie, J. A. Zeitler, and S. Hofmann, "Contactless graphene conductivity mapping on a wide range of substrates with terahertz time-domain reflection spectroscopy," Sci. Rep. **7**, 1–9 (2017).
8. D. M. A. Mackenzie, P. R. Whelan, P. Bøggild, P. U. Jepsen, A. Redo-Sanchez, D. Etayo, N. Fabricius, and D. H. Petersen, "Quality assessment of terahertz time-domain spectroscopy transmission and reflection modes for graphene conductivity mapping," Opt. Express **26**(7), 9220–9229 (2018).
9. X. Li, Y. Zhu, W. Cai, M. Borysiak, B. Han, D. Chen, R. D. Piner, L. Colombo, and R. S. Ruoff, "Transfer of large-area graphene films for high-performance transparent conductive electrodes," Nano Lett. **9**(12), 4359–4363 (2009).
10. S. Bae, H. Kim, Y. Lee, X. Xu, J.-S. Park, Y. Zheng, J. Balakrishnan, T. Lei, H. R. Kim, Y. I. Song, Y.-J. Kim, K. S. Kim, B. Özyilmaz, J.-H. Ahn, B. H. Hong, and S. Iijima, "Roll-to-roll production of 30-inch graphene films for transparent electrodes," Nat. Nanotechnol. **5**(8), 574–578 (2010).
11. Y. Lee, S. Bae, H. Jang, S. Jang, S.-E. Zhu, S. H. Sim, Y. I. Song, B. H. Hong, and J.-H. Ahn, "Wafer-scale synthesis and transfer of graphene films," Nano Lett. **10**(2), 490–493 (2010).
12. S. R. Na, J. W. Suk, L. Tao, D. Akinwande, R. S. Ruoff, R. Huang, and K. M. Liechti, "Selective mechanical transfer of graphene from seed copper foil using rate effects," ACS Nano **9**(2), 1325–1335 (2015).
13. L. Gao, W. Ren, H. Xu, L. Jin, Z. Wang, T. Ma, L.-P. Ma, Z. Zhang, Q. Fu, L.-M. Peng, X. Bao, and H.-M. Cheng, "Repeated growth and bubbling transfer of graphene with millimetre-size single-crystal grains using platinum," Nat. Commun. **3**(1), 699 (2012).
14. S. Y. Yang, J. G. Oh, D. Y. Jung, H. Choi, C. H. Yu, J. Shin, C. G. Choi, B. J. Cho, and S. Y. Choi, "Metal-etching-free direct delamination and transfer of single-layer graphene with a high degree of freedom," Small **11**(2), 175–181 (2015).
15. P. R. Whelan, B. S. Jessen, R. Wang, B. Luo, A. C. Stoot, D. M. A. Mackenzie, P. Braeuninger-Weimer, A. Jouvray, L. Prager, L. Camilli, S. Hofmann, P. Bøggild, and T. J. Booth, "Raman spectral indicators of catalyst decoupling for transfer of CVD grown 2D materials," Carbon **117**, 75–81 (2017).
16. R. Wang, P. R. Whelan, P. Braeuninger-Weimer, S. Tappertzhofen, J. A. Alexander-Webber, Z. A. Van Veldhoven, P. R. Kidambi, B. S. Jessen, T. Booth, P. Bøggild, and S. Hofmann, "Catalyst Interface Engineering for Improved 2D Film Lift-Off and Transfer," ACS Appl. Mater. Interfaces **8**(48), 33072–33082 (2016).
17. P. U. Jepsen, J. K. Jensen, and U. Møller, "Characterization of aqueous alcohol solutions in bottles with THz reflection spectroscopy," Opt. Express **16**(13), 9318–9331 (2008).
18. D. M. A. Mackenzie, J. D. Buron, P. R. Whelan, J. M. Caridad, M. Bjergfelt, B. Luo, A. Shivayogimath, A. L. Smitshuysen, J. D. Thomsen, T. J. Booth, L. Gammelgaard, J. Zultak, B. S. Jessen, P. Bøggild, and D. H. Petersen, "Quality assessment of graphene: Continuity, uniformity, and accuracy of mobility measurements," Nano Res. **10**(10), 1–10 (2017).
19. L. J. van der Pauw, "A method of measuring specific resistivity and Hall effect of discs of arbitrary shape," Philips Res. Reports **13**, 1–11 (1958).
20. J. D. Buron, F. Pizzocchero, B. S. Jessen, T. J. Booth, P. F. Nielsen, O. Hansen, M. Hilke, E. Whiteway, P. U. Jepsen, P. Bøggild, and D. H. Petersen, "Electrically continuous graphene from single crystal copper verified by terahertz conductance spectroscopy and micro four-point probe," Nano Lett. **14**(11), 6348–6355 (2014).
21. P. R. Whelan, K. Iwaszczuk, R. Wang, S. Hofmann, P. Bøggild, and P. U. Jepsen, "Robust mapping of electrical properties of graphene from terahertz time-domain spectroscopy with timing jitter correction," Opt. Express **25**(3), 2725–2732 (2017).
22. D. M. A. Mackenzie, J. D. Buron, P. Bøggild, P. U. Jepsen, and D. H. Petersen, "Contactless graphene conductance measurements: the effect of device fabrication on terahertz time-domain spectroscopy," Int. J. Nanotechnol. **13**(8/9), 591 (2016).
23. J. Náhlík, I. Kašpárková, and P. Fitl, "Study of quantitative influence of sample defects on measurements of resistivity of thin films using van der Pauw method," Measurement **44**(10), 1968–1979 (2011).

1. Introduction

As chemical vapor deposition growth (CVD) of graphene is reaching industrial maturity, reliable large-area characterization of the electrical properties of graphene on a wide range of substrates is becoming a necessary requirement [1]. Terahertz time-domain spectroscopy (THz-TDS) has proven useful as a fast non-contact method for extracting the conductivity, carrier scattering time, and mobility of graphene on highly resistive silicon (Si) substrates through transmission-mode measurements [2–6]. Recently, the conductivity of graphene on Si has also been extracted from reflection-mode THz-TDS, which avoids the requirement of the Si substrate to be highly resistive [7,8].

For applications where the substrate needs to be mechanically flexible, it is necessary to be able to measure the electrical properties non-destructively on other substrates than Si, such as for instance polymeric films. The ability to map the key electrical properties of graphene on polymeric films would also be beneficial for process optimization of graphene transfers,

Optics EXPRESS

since most transfer methods utilize a polymer as handling layer during the transfer process [9–16].

Here, we use THz-TDS to measure the electrical properties of graphene on polyethylene terephthalate (PET) films, which are widely used as substrates for graphene devices. We show that the conductivity extracted from THz-TDS measurements is comparable to measurements conducted by four point probe (4pp) measurements. In order to show the amenability of THz-TDS as a characterization tool for large-scale sheet-based or roll-to-roll processing, we present conductivity maps of 25x30 cm^2 area graphene on PET. Additionally, the THz-TDS measurements highlight large defects such as tears and scratches in the graphene layer on polymeric substrates, which are difficult to assess by optical microscopy, in particular on transparent substrates.

2. Methods

Graphene was grown on copper foil by chemical vapor deposition (CVD) in a low pressure tube furnace system (40 cm diameter, 300 cm length) equipped with a distributed multi-function chamber system which can precisely control graphene growth parameters such as temperature, vacuum, and gas concentration. Prior to growth, the 25 μm thick copper foil was washed subsequently with acetone, ethanol and deionized (DI) water to remove any organic impurities. The cleaned copper foils were immersed in 1 wt% sulfuric acid for 3 minutes to remove surface oxides and then thoroughly rinsed with DI water. The copper foils were cut to 25x30 cm^2, placed in the quartz tube chamber and annealed at 1000 °C with 1000 sccm Ar and 500 sccm H_2 to remove residuals on the copper surface. During the CVD growth, the H_2 gas was kept at 500 sccm and CH_4 was added at 100 sccm for 30 minutes. After growth, CH_4 and H_2 were turned off and the copper/graphene was auto-delivered out under Ar gas protection.

The as-grown graphene on copper was laminated on a thermal release tape (Nitto NO.319Y-4LS RL) using a roller machine. The tape/graphene/copper film was put into a 2 M aqueous solution of $(NH_4)_2S_2O_8$ to remove the copper and subsequently washed with DI water several times before drying with N_2. The tape/graphene film was put into a 0.025 M $AuCl_3/H_2O$ solution for 1 minute, then dried with N_2 and laminated onto PET film. Finally, the thermal release tape was released at 140 °C.

THz-TDS measurements were performed using a commercial fiber-coupled spectrometer described in detail elsewhere [5]. The samples consisting of graphene on PET were raster scanned in the focal plane of the THz beam at normal incidence to form a spatial map with a resolution of ~1 mm at 1 THz. Each measurement point in the collected maps consists of an average of 40 waveforms. The frequency-dependent sheet conductivity of graphene, $\tilde{\sigma}_s(\omega) = \sigma_1 + i\sigma_2$, is calculated from each measurement point in a scanned map from the transmission function $\tilde{T}_{film}(\omega) = \tilde{E}_{film}(\omega) / \tilde{E}_{sub}(\omega)$ where $\tilde{E}_{film}(\omega)$ and $\tilde{E}_{sub}(\omega)$ are the Fourier transforms of the THz waveforms transmitted through graphene covered PET and non-graphene covered PET, respectively. For the PET substrate we use a complex refractive index, *n* [17].

The sheet resistance of 1x1 cm^2 graphene on PET samples was measured by 4pp measurements with probe contacts at the corners of the samples. Measurements were conducted in two configurations (A and C) [18] in order to extract the van der Pauw (vdP) sheet resistance [19]. The resistance values of the individual measurements (R_A and R_C) are used for error bars. Sheet resistance measurements on a 25x30 cm^2 graphene on PET sample were conducted using a commercial RTS-9 Probes Tech 4pp system.

3. Results and discussion

The sheet conductivity of graphene on ~500 μm thick high-resistivity Si is routinely determined from THz-TDS measurements by isolating the signal from one of the transients

Optics EXPRESS

from internal reflections in the substrate [Fig. 1(a)] by time-windowing [5,20,21]. The time between internal reflections in the PET substrate is much lower compared to standard Si substrates due to reduced thickness (~225 μm in this case) and a lower refractive index at THz frequencies (~1.75). Therefore, the transients from the internal reflections are all combined in a single transient as shown in Fig. 1a. $\tilde{E}_{film}(\omega)$ and $\tilde{E}_{sub}(\omega)$ contain terms from the directly transmitted pulse together with all the following echoes from internal reflections. The expressions for $\tilde{E}_{film}(\omega)$ and $\tilde{E}_{sub}(\omega)$ in such a case are

$$\tilde{E}_{film}(\omega) = E_0 \tilde{t}_{film} \tilde{t}_{sub,air} e^{-i\delta} \sum_{n=0}^{\infty} (\tilde{r}_{sub,air} \tilde{r}_{film} e^{-i2\delta})^n = \frac{E_0 \tilde{t}_{film} \tilde{t}_{sub,air} e^{-i\delta}}{1 - \tilde{r}_{sub,air} \tilde{r}_{film} e^{-i2\delta}}, \quad (1)$$

$$\tilde{E}_{sub}(\omega) = E_0 \tilde{t}_{air,sub} \tilde{t}_{sub,air} e^{-i\delta} \sum_{n=0}^{\infty} (\tilde{r}^2_{sub,air} e^{-i2\delta})^n = \frac{E_0 \tilde{t}_{air,sub} \tilde{t}_{sub,air} e^{-i\delta}}{1 - \tilde{r}^2_{sub,air} e^{-i2\delta}}, \quad (2)$$

where $\delta = \omega dn / c$ with substrate thickness d. The infinite sums were simplified by the geometric series $1 + x + x^2 + x^3 + ... = 1/(1-x)$ for abs(x) < 1. The transmission coefficient from air to a substrate covered by a thin conducting film is $\tilde{t}_{film}(\omega) = 2/(n+1+Z_0\tilde{\sigma}_s(\omega))$ [2], where Z_0 = 377 Ω is the vacuum impedance. Similarly, the reflection coefficient inside a substrate covered by a thin conducting film is $\tilde{r}_{film}(\omega) = (n-1-Z_0\tilde{\sigma}_s(\omega))/(n+1+Z_0\tilde{\sigma}_s(\omega))$ [1]. The transmission $\tilde{t}$ and $\tilde{r}$ reflection coefficients between air and non-graphene covered substrate are given by the Fresnel equations. The sheet conductivity can following be determined from the transmission function as

$$\tilde{\sigma}_s(\omega) = \frac{n_A^2 - n_B^2 e^{-i\delta} + (n_B^2 e^{-i\delta} - n_A^2)\tilde{T}_{film}(\omega)}{(n_A + n_B^2 e^{-i\delta}) Z_0 \tilde{T}_{film}(\omega)}, \quad (3)$$

where $n_A = n+1$ and $n_B = n-1$. The DC sheet conductance, σ_{DC}, and the carrier scattering time, τ, can be found by fitting the real part of the frequency dependent sheet conductivity, σ_1, to the Drude model [6]

$$\tilde{\sigma}_s(\omega) = \frac{\sigma_{DC}}{1 - i\omega\tau}. \quad (4)$$

Examples of Drude fits to σ_1 for graphene on PET are shown in Fig. 1(b). The small peak in the conductivity seen at ~0.9 THz is likely to originate from minute thickness variations in the PET substrate. The uncertainties shown for σ_{DC} and τ are standard errors from the fit. It is noted that the uncertainty on the scattering time is always higher than that of the DC sheet conductance. Figure 1(b) also highlights the necessity of treating the signal as a combination of the directly transmitted and internally reflected transients. The extracted sheet conductivity is seen to have a highly oscillatory appearance if we consider the signal as only consisting of a directly transmitted transient [20,21], which would increase the uncertainty on parameters extracted by fitting to the Drude model [Eq. (4)].

Optics EXPRESS

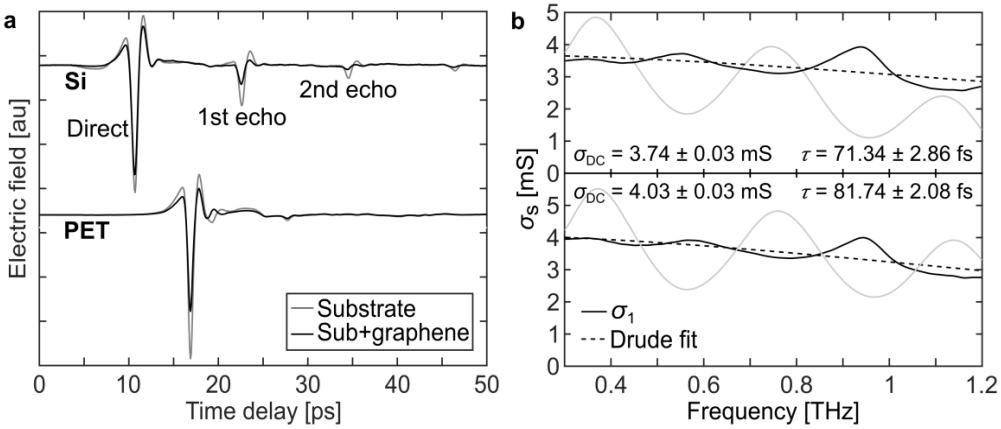

Fig. 1. (a) Waveforms of THz pulses after transmission through Si and PET substrates without and with graphene. (b) Black lines show two examples of representative sheet conductivity spectra for graphene on PET extracted from Eq. (3) together with fits to the Drude model [Eq. (4)]. Grey lines show the sheet conductivity extracted by considering the signal as only consisting of a directly transmitted transient.

THz-TDS was used to map 1x1 cm^2 samples of graphene on PET with 200 μm stepsize. An example of a conductivity map is shown in Fig. 2(a). The frequency dependent sheet conductivity of the central 20x20 measurement points (in order to avoid artifacts from the sample edges [22]) was fitted by the Drude model in order to extract σ_{DC}. The sheet resistance, R_s, was defined in each point as $1/\sigma_{DC}$. An R_s histogram with the 400 measurement values is shown in Fig. 2(b). An average R_s of 273 ± 9 Ω was determined as the mean from a generalized extreme value (GEV) distribution fitted to the histogram (black curve). The sample is electrically homogeneous with a standard deviation of less than 3.5% of the average value.

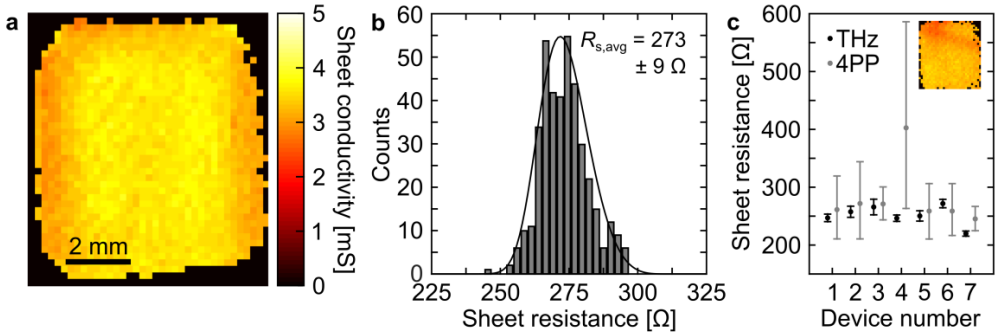

Fig. 2. (a) THz-TDS sheet conductivity map of σ_1 averaged from 0.3 to 1.2 THz for a 1x1 cm^2 sample of graphene on PET. (b) Histogram of sheet resistance values from the central 20x20 measurement points for the sample in (a) with a fitted GEV distribution shown as black curve. (c) Comparison of sheet resistance measured by THz-TDS and 4pp measurements for 7 1x1 cm^2 graphene on PET samples. Inset shows the THz conductivity map (same size and scale as in (a)) for sample 4 with a scratch affecting the 4pp measurement.

In order to validate the R_s values obtained from THz-TDS measurements of graphene on PET, we conducted 4pp measurements on 7 individual 1×1 cm^2 samples in order to obtain the vdP-corrected sheet resistance. Figure 2(c) shows the sheet resistance obtained from the 4pp measurements compared to the R_s values extracted from the central 20x20 THz-TDS measurement points on the same samples. There is a good agreement between the 4pp and THz-TDS measurements except for device 4, which also clearly has a scratch across the sample [Fig. 2(c), inset]. Such a scratch will have a big impact on the 4pp measurement as the

Optics EXPRESS

current flow between source and drain electrodes is affected by macroscopic disruptions [23], while the THz-TDS measurement is representing the average conductivity of the graphene covered region, and is far less sensitive to large-scale electrical discontinuity [1].

A 25x30 cm^2 area of graphene on PET was mapped with 1 mm stepsize by THz-TDS. Figure 3(a) shows a photograph of the sample together with the conductivity map. The sample generally seems to be homogeneously conducting except for a region in one side that appears to be scratched. The scratched region is easily identified from the THz conductivity map, while it is not easily visible by optical inspection of the sample.

We extracted σ_{DC} and τ from each of the 34608 measurement points inside the dotted rectangle in Fig. 3(a). Histograms of R_s and τ are shown in Figs. 3(b) and 3(c). From a fitted GEV distribution we find an average R_s of 234 ± 4 Ω. The low standard deviation (~1.7%) indicates a very high homogeneity across the whole sample. From a fitted normal distribution we find an average τ of 68.5 ± 5.6 fs.

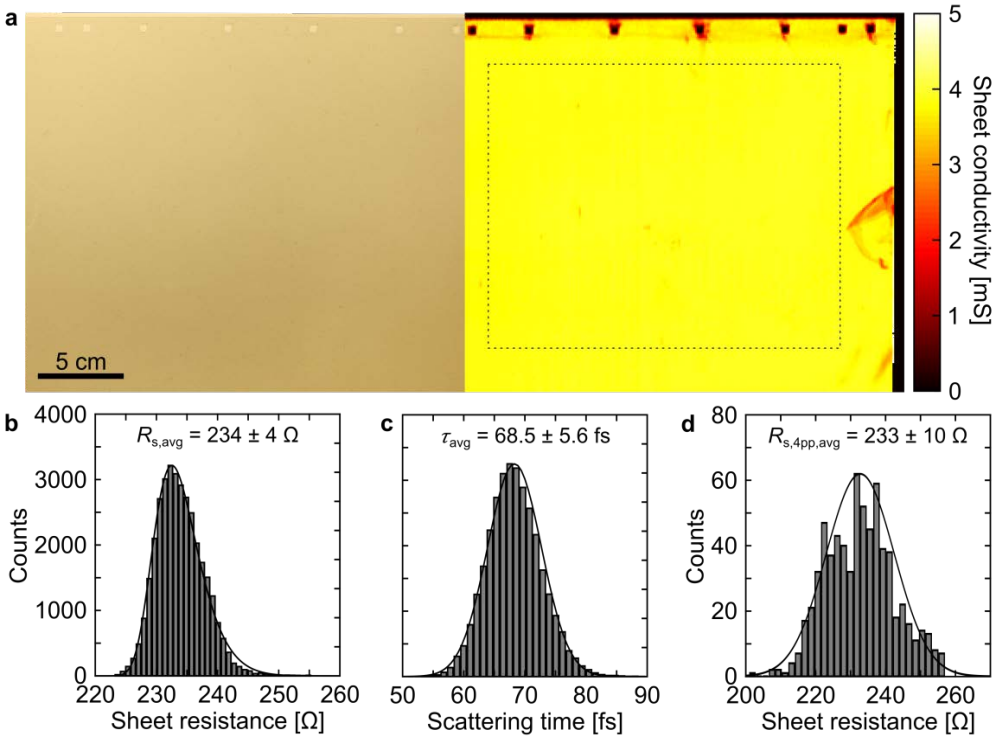

Fig. 3. (a) Photograph of a 25x30 cm^2 graphene on PET sample combined with the THz-TDS sheet conductivity map of σ_1 (mirrored) averaged from 0.3 to 1.2 THz. Dotted square highlights the 206x168 measurement points used for extracting the electrical properties in (b-c) showing histograms of (b) sheet resistance with a fitted GEV distribution and (c) carrier scattering time with a fitted normal distribution using the same counts on y-axis as in (b). (d) Sheet resistance histogram with a fitted normal distribution of 690 points measured by 4pp on a 25x30 cm^2 sample similar to the one shown in (a).

A 25x30 cm^2 sample of graphene on PET grown and transferred similarly to the one shown in Fig. 3(a) was characterized by 4pp measurements. The 4pp measurements were conducted with 1 cm stepsize across the sample with a histogram of the corresponding $R_{s,4pp}$ values shown in Fig. 3(d). The average $R_{s,4pp}$ of 233 ± 10 Ω is in good agreement with the values we find from THz-TDS measurements on a similar sample highlighting both the ability of extracting R_s from graphene on polymer films by THz-TDS and the homogeneity of subsequent growth, transfer, and doping processes.

Optics EXPRESS

The easy identification of scratches in graphene on PET samples observed in THz-TDS maps is further highlighted in Fig. 4. A sample was transported in a plastic box with indentations for holding the sample. Lines of lower conductivity with a period corresponding to the distance between indentations in the packaging are clearly visible, which emphasizes the value of THz-TDS as an efficient metrology tool for characterization of graphene on polymeric films.

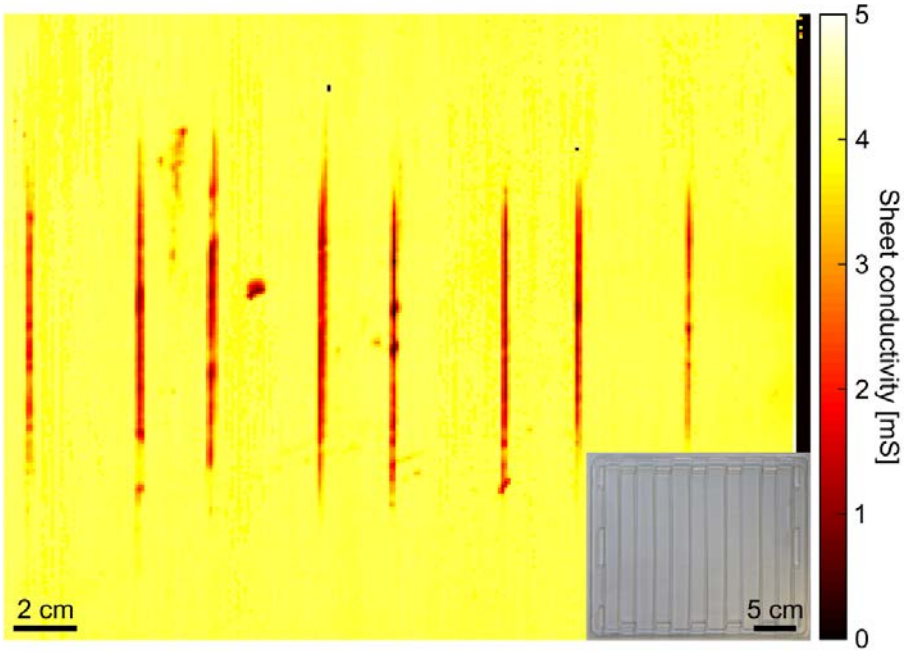

Fig. 4. THz-TDS sheet conductivity map of σ_1 averaged from 0.3 to 1.2 THz for a 25x30 cm^2 graphene on PET sample that has been damaged during transport. The bottom right inset shows a photograph of the box used for packaging with indentations for holding the sample.

4. Conclusion

We have shown that THz-TDS can be used to reliably extract the conductivity of graphene on polymeric films. This greatly extends the scope and application space of non-contact electrical mapping, and provides a clear starting point for systematic optimization and consistent fabrication of large-area graphene for flexible applications, with the path towards inline process monitoring cleared. The technique has the added feature that the graphene can be measured at intermediate steps in a process, since it is non-destructive and non-contact. This is a crucial point, since testing of encapsulated films upon environmental stress factors such as changes in ambient conditions or repeated cycles of mechanical straining or bending, can be done with a high spatial resolution multiple times during such testing, to reveal the exact origin of failure and provide a deeper understanding of the interplay between the different layers in a compound material or film.

Funding

Danish National Research Foundation (DNRF) Center for Nanostructured Graphene (DNRF103); EU Graphene Flagship Core 1 (696656); EU-FP7 Gladiator (604000); Innovation Fund Denmark project DA-GATE (12-131827); Natural Science Foundation of the People's Republic of China (NSFC) (51402291, 51702315); Chongqing Research Program of Basic Research: Frontier Technology (cstc2015jcyjA50018)